

BEVTrack: A Simple Baseline for 3D Single Object Tracking in Bird’s-Eye View

Yuxiang Yang¹, Yingqi Deng¹, Jiahao Nie¹, Jing Zhang²

¹ School of Electronics and Information, Hangzhou Dianzi University, Hangzhou 310018, China

² School of Computer Science, The University of Sydney, NSW 2006, Australia

{yyx, den, jhnie}@hdu.edu.cn; jing.zhang1@sydney.edu.au

Abstract

3D single object tracking (SOT) in point clouds is still a challenging problem due to appearance variation, distractors, and high sparsity of point clouds. Notably, in autonomous driving scenarios, the target object typically maintains spatial adjacency across consecutive frames, predominantly moving horizontally. This spatial continuity offers valuable prior knowledge for target localization. However, existing trackers, which often employ point-wise representations, struggle to efficiently utilize this knowledge owing to the irregular format of such representations. Consequently, they require elaborate designs and solving multiple subtasks to establish spatial correspondence. In this paper, we introduce BEVTrack, a simple yet strong baseline framework for 3D SOT. After converting consecutive point clouds into the common Bird’s-Eye View representation, BEVTrack inherently encodes spatial proximity and adeptly captures motion cues for tracking via a simple element-wise operation and convolutional layers. Additionally, to better deal with objects having diverse sizes and moving patterns, BEVTrack directly learns the underlying motion distribution rather than making a fixed Laplacian or Gaussian assumption as in previous works. Without bells and whistles, BEVTrack achieves state-of-the-art performance on KITTI and NuScenes datasets while maintaining a high inference speed of 122 FPS. The code will be released at [BEVTrack](https://github.com/yyx9813/BEVTrack).

1. Introduction

3D single object tracking (SOT) is crucial for various applications, such as autonomous driving. It aims to localize a specific target across a sequence of point clouds, given only its initial status. Existing approaches [20, 26] commonly rely on point-wise representation for tracking, directly taking raw point clouds as input. For example, after extracting features using a shared point-based backbone [19, 23], P2B [20] and its follow-up works [7, 8, 15, 22, 24, 25, 27] identify the target points with a point-wise appearance matching technique, and then localize the tar-

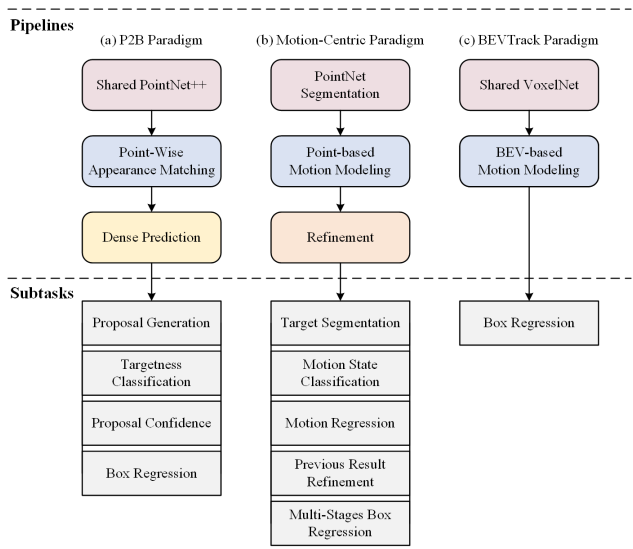


Figure 1. Comparison with typical 3D SOT paradigms. (a) P2B Paradigm [20]. (b) Motion-Centric Paradigm [26]. (c) Our BEV representation-based paradigm.

get with a dense prediction head such as Region Proposal Network [17], as illustrated in Fig. 1(a). Differently, M2-Track [26] proposes a motion-centric paradigm. It first identifies the target points with a PointNet [18] segmentation network. After that, the target location is estimated through a motion modeling approach followed by a refinement module, as illustrated in Fig. 1(b).

Due to factors such as variations in appearance, the presence of distractors, and the sparsity of point clouds, it is challenging to localize the target. In autonomous driving scenarios, we observe that the target object typically maintains spatial adjacency across consecutive frames, predominantly moving horizontally [10]. This spatial continuity offers valuable prior knowledge for target localization. Although trackers based on point-wise representations have exhibited superior performance in tracking benchmarks, the irregular format of such representations makes them inefficient in utilizing this spatial knowledge. Consequently,

these trackers necessitate elaborate designs [8, 24, 27] and the resolution of multiple subtasks [20, 26] to establish spatial correspondence between objects and predict their locations, resulting in complex tracking frameworks and increased challenges in hyper-parameter tuning.

In this paper, we present BEVTrack, a simple yet strong baseline framework for 3D SOT, as shown in Fig. 1(c). By converting unordered point clouds into the common Bird’s-Eye View (BEV) representation [6, 12, 13, 16], BEVTrack inherently encodes spatial proximity and adeptly captures motion cues for tracking. Specifically, it directly takes point clouds from two consecutive frames as input, preserving contextual information [24] without the need for sampling or cropping, and employs VoxelNet [29] as a shared backbone to extract geometric features of the point clouds in parallel. Subsequently, we squeeze the sparse 3D features along the height dimension to obtain BEV features. Given that corresponding objects are adjacent in the BEV representation, we effectively fuse them together using element-wise operations and convolutional layers to capture motion cues. Finally, we employ a multilayer perceptron (MLP) to predict the target’s location, resulting in a simple one-stage tracking pipeline.

To train the regression-based trackers, current approaches typically employ conventional L1 or L2 losses. These kinds of supervision implicitly assume Gaussian or Laplace distributions with constant variances for object locations (*e.g.*, offsets), which is inflexible in dealing with objects of varying sizes and diverse moving patterns. To address this issue, we advocate the direct learning of underlying distributions [2, 11] specific to distinct object classes, thereby introducing a novel distribution-aware regression strategy. This strategy provides more accurate guidance for tracking and improves tracking performance, all while avoiding additional computational overhead during inference. Despite no elaborate design, BEVTrack exhibits a substantial performance advantage over the current state-of-the-art (SOTA) methods on challenging tracking datasets, *i.e.*, KITTI [4] and NuScenes [1], while running at real-time (about 122 FPS) on a single NVIDIA RTX4090 GPU.

The main contributions of this paper are three-fold:

- We propose BEVTrack, a simple yet strong baseline framework for 3D SOT. This pioneering approach efficiently leverages spatial information through BEV representation, resulting in a simplified tracking pipeline design.
- We present a novel distribution-aware regression strategy, which directly learns the underlying motion distributions for objects of varying sizes and diverse moving patterns. This strategy provides accurate guidance for tracking, resulting in improved performance while avoiding extra computational overhead.
- BEVTrack achieves SOTA performance on two popular benchmarks while maintaining a high inference speed.

2. Method

2.1. Overview

Given the 3D bounding box (BBox) of a specific target at the initial frame, 3D SOT aims to localize the target by predicting its 3D BBoxes in the subsequent frames. A 3D BBox $\mathcal{B}_t \in \mathbb{R}^7$ is parameterized by its center (*i.e.*, x, y, z coordinates), orientation (*i.e.*, heading angle θ around the *up*-axis), and size (*i.e.*, width, length, and height). Suppose the point clouds in two consecutive frames are denoted as $\mathcal{P}_{t-1} \in \mathbb{R}^{N_{t-1} \times 3}$ and $\mathcal{P}_t \in \mathbb{R}^{N_t \times 3}$, respectively, where N_{t-1} and N_t are the numbers of points in the point clouds. At timestamp t , we take all points in the \mathcal{P}_{t-1} and those points in the \mathcal{P}_t within the search region as input, without sampling or cropping. Since the tracking target has a small change in size and orientation, we assume constant target size and orientation. Thus, we only regress the inter-frame target translation (*i.e.*, $\Delta x, \Delta y, \Delta z$) to simplify the tracking task. By applying the translation to the 3D BBox \mathcal{B}_{t-1} , we can compute the 3D BBox \mathcal{B}_t to localize the target in the current frame. The tracking process can be formulated as:

$$\mathcal{F}(\mathcal{P}_{t-1}, \mathcal{P}_t) \mapsto (\Delta x, \Delta y, \Delta z), \quad (1)$$

where \mathcal{F} is the mapping function learned by the tracker.

Following Eq. (1), we propose BEVTrack, a simple yet strong baseline framework for 3D SOT. The overall architecture of BEVTrack is presented in Fig. 2. It first utilizes a shared VoxelNext [29] to extract 3D features, and then squeeze them to obtain the BEV representation. Subsequently, BEVTrack fuses the BEV features via concatenation and several convolutional layers and regresses the target translation via an MLP. For accurate regression, we employ a novel distribution-aware regression strategy to optimize BEVTrack during training.

2.2. Feature Extraction

First, we need to learn discriminative features for describing the raw point clouds. Instead of adopting point-based backbone [18, 19, 23] as in previous works [20, 24, 26], we propose to utilize VoxelNet [29] for feature extraction, which can capture 3D shape information of the object. Therefore the potential target can be identified from the background in sparse point clouds.

Given two raw point clouds from consecutive frames, through the dynamic voxelization process [28], we convert the unordered points into evenly spaced grids. After that, the shared VoxelNet backbone stacked by sparse convolutions [21] processes the features of non-empty voxels and yields the sparse 3D features, where the initial feature of each voxel is simply calculated as the mean values of point coordinates (*i.e.*, x, y, z) within each voxel [29]. Finally, we squeeze the sparse 3D features along the height dimension to derive the BEV features $\mathcal{B}_{t-1} \in \mathbb{R}^{H \times W \times C}$ and

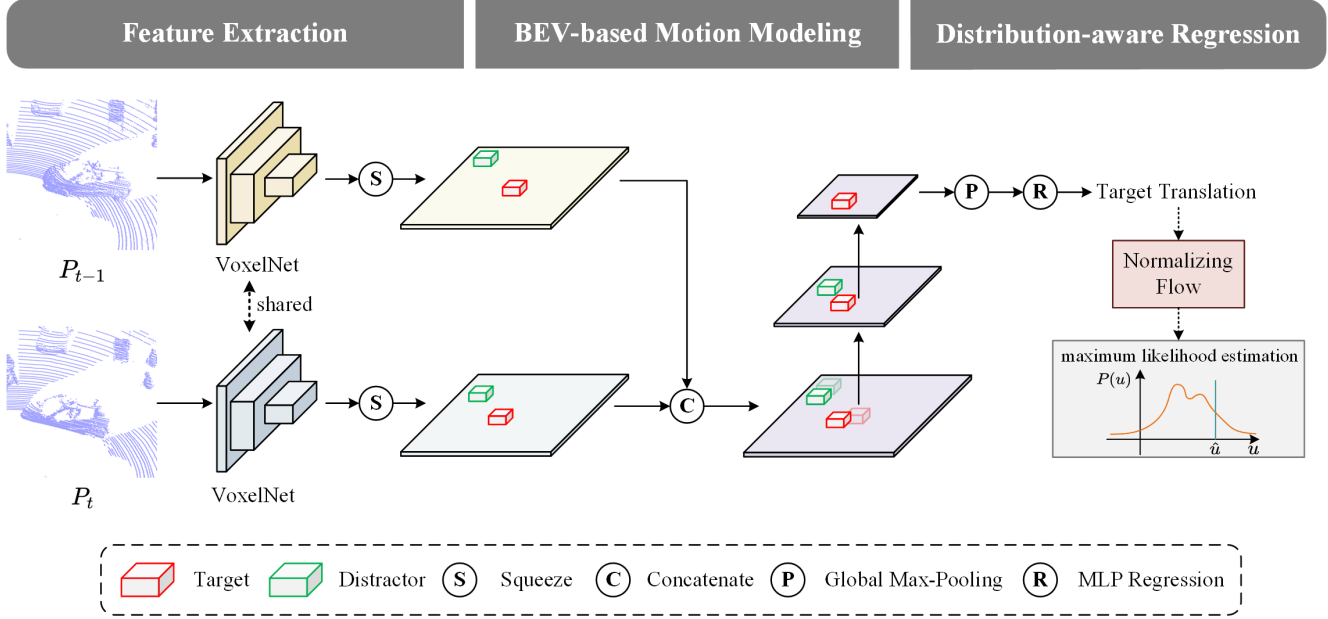


Figure 2. **Diagram of BEVTrack.** It employs VoxelNet to extract features from consecutive frames, which are further transformed into BEV representation. Then, it fuses the BEV features and captures motion clues via concatenation and several convolutional layers. Finally, it regresses motion offsets via an MLP. During training, we propose a distribution-aware regression strategy to optimize BEVTrack.

$\mathcal{B}_t \in \mathbb{R}^{H \times W \times C}$, where H and W denote the 2D grid dimension and C is the number of feature channels.

2.3. BEV-based Motion Modeling

Given the BEV features \mathcal{B}_{t-1} and \mathcal{B}_t , BEV-based Motion Modeling (BMM) aims to encode spatial proximity and capture motion cues in BEV. Since objects present in \mathcal{B}_{t-1} and \mathcal{B}_t are spatially adjacent, we can easily fuse them together with an element-wise operator such as concatenation to preserve their spatial proximity. Subsequently, the resulting concatenated feature is fed into several convolutional blocks, each comprising three convolutional layers with a stride of 1 or 2. This module reduces the spatial dimensions of the fused BEV feature, allowing it to effectively capture a wide range of motion patterns, including both small and large movements. The above process can be formulated as:

$$\mathcal{F} = \text{Conv}([\mathcal{B}_{t-1}; \mathcal{B}_t]), \quad (2)$$

where Conv denotes the convolutional blocks in BMM and $[;]$ denotes the concatenation operator. $\mathcal{F} \in \mathbb{R}^{H' \times W' \times C'}$, where H' , W' , and C' denote the spatial dimension and the number of feature channels, respectively.

Finally, we employ a max-pooling layer and an MLP to predict the target translation offset, *i.e.*,

$$\mathcal{C} = \text{MLP}(\text{Pool}(\mathcal{F})), \quad (3)$$

where $\mathcal{C} \in \mathbb{R}^6$ denotes the expectation of the target translation offset $\bar{u} \in \mathbb{R}^3$ and the standard deviation $\sigma \in \mathbb{R}^3$,

which will be detailed in Sec.2.4. By applying the translation to the last state of the target, we can localize the target in the current frame.

2.4. Distribution-aware Regression

In previous works, it is often to employ conventional L1 or L2 losses for target location regression during training, which indeed makes a fixed Laplacian or Gaussian assumption about the distribution of target location. In contrast to them, we propose to directly learn the underlying motion distribution and introduce a novel distribution-aware regression strategy. In this way, it can provide more accurate guidance for tracking and BEVTrack can better deal with objects having diverse sizes and moving patterns.

Following [11], we model the distribution of target translation offset $u \sim P(u)$ with reparameterization. Specifically, $P(u)$ can be obtained by scaling and shifting z from a zero-mean distribution $z \sim P_Z(z)$ with transformation function $u = \bar{u} + \sigma \cdot z$, where \bar{u} denotes the expectation of target translation offset and σ denotes the scale of the distribution. $P_Z(z)$ can be modeled by a normalizing flow model (*e.g.*, real NVP [2]). Given this transformation function, the density function of $P(u)$ can be calculated as:

$$\log P(u) = \log P_Z(z) - \log \sigma. \quad (4)$$

In contrast to prior methods that solely regressed the deterministic target translation offset u , our method focuses on regressing two distinct parameters: the expectation of target translation offset \bar{u} and its standard deviation σ .

In this work, we employ residual log-likelihood estimation (RLE) in [11] to estimate the above parameters. RLE factorizes the distribution $P_Z(z)$ into one prior distribution $Q_Z(z)$ (e.g., Laplace distribution or Gaussian distribution) and one learned distribution $G_Z(z | \theta)$. To maximize the likelihood in Eq. (4), we can minimize the following loss:

$$L_{\text{regression}} = -\log Q_Z(\hat{z}) - \log G_Z(\hat{z} | \theta) + \log \sigma. \quad (5)$$

Here, $\hat{z} = (\hat{u} - \bar{u})/\sigma$, \hat{u} is the ground truth translation offset.

3. Experiment

3.1. Experimental Settings

Datasets. We validate the effectiveness of BEVTrack on two widely-used challenging datasets: KITTI [4], and NuScenes [1]. KITTI contains 21 video sequences for training and 29 video sequences for testing. We follow previous work [20] to split the training set into train/val/test splits due to the inaccessibility of the labels of the test set. NuScenes contains 1,000 scenes, which are divided into 700/150/150 scenes for train/val/test. Following the implementation in [25], we compare with the previous methods on five categories including Car, Pedestrian, Truck, Trailer, and Bus.

Evaluation Metrics. Following [20], we adopt Success and Precision defined in one pass evaluation (OPE) [9] as the evaluation metrics. Success denotes the Area Under Curve (AUC) for the plot showing the ratio of frames where the Intersection Over Union (IoU) between the predicted box and the ground truth is larger than a threshold, ranging from 0 to 1, while Precision denotes the AUC for the plot showing the ratio of frames where the distance between their centers is within a threshold, ranging from 0 to 2 meters.

3.2. Comparison with State-of-the-art Methods

Results on KITTI. We present a comprehensive comparison of BEVTrack with the previous state-of-the-art approaches on KITTI, namely SC3D [5], P2B [20], 3DSiamRPN [3], BAT [25], PTT [22], V2B [7], PTTR [27], GLT-T [15], OSP2B [14], STNet [8], M2-Track [26], and CXTrack [24]. As shown in Table 1, BEVTrack achieves the best performance across all categories, with the exception of the 'Car' category, where it is marginally surpassed by STNet (*i.e.*, 72.1/84.0 v.s. 71.2/83.4).

Results on NuScenes. We compare BEVTrack with six representative trackers, namely SC3D [5], P2B [20], BAT [25], GLT-T [15], PTTR [27], and M2-Track [26], on NuScenes. As shown in Table 2, our BEVTrack consistently outperforms the prior state-of-the-art technique, *i.e.*, the

Table 1. **Comparisons with state-of-the-art methods on KITTI dataset.** Success/Precision are used for evaluation. **Bold** and underline denote the best and the second-best scores, respectively.

Method	Car (6424)	Pedestrian (6088)	Van (1248)	Cyclist (308)	Mean (14068)
SC3D	41.3/57.9	18.2/37.8	40.4/47.0	41.5/70.4	31.2/48.5
P2B	<u>56.2</u> /72.8	28.7/49.6	40.8/48.4	32.1/44.7	42.4/60.0
3DSiamRPN	58.2/76.2	35.2/56.2	45.7/52.9	36.2/49.0	46.7/64.9
BAT	60.5/77.7	42.1/70.1	52.4/67.0	33.7/45.4	51.2/72.8
PTT	67.8/81.8	44.9/72.0	43.6/52.5	37.2/47.3	55.1/74.2
V2B	70.5/81.3	48.3/73.5	50.1/58.0	40.8/49.7	58.4/75.2
PTTR	65.2/77.4	50.9/81.6	52.5/61.8	65.1/90.5	57.9/78.1
GLT-T	68.2/82.1	52.4/78.8	52.6/62.9	68.9/92.1	60.1/79.3
OSP2B	67.5/82.3	53.6/85.1	56.3/66.2	65.6/90.5	60.5/82.3
STNet	72.1 / <u>84.0</u>	49.9/77.2	58/70.6	73.5/93.7	61.3/80.1
M2-Track	65.5/80.8	61.5/88.2	53.8/70.7	73.2/93.5	62.9/83.4
CXTrack	69.1/81.6	<u>67.0</u> / <u>91.5</u>	60.0/71.8	74.2/94.3	67.5/ <u>85.3</u>
BEVTrack	<u>71.2</u> / <u>83.4</u>	68.4 / 94.0	63.3 / <u>75.7</u>	74.6 / 94.7	69.4 / 87.6
Improvement	<u>10.9</u> / <u>0.6</u>	<u>11.4</u> / <u>2.5</u>	<u>13.3</u> / <u>13.9</u>	<u>10.4</u> / <u>0.4</u>	<u>11.9</u> / <u>2.3</u>

point-wise representation-based M2-Track, by a significant margin. This remarkable improvement can be attributed to BEVTrack’s adept utilization of spatial information based on the BEV representation, making it particularly effective in scenarios characterized by substantial appearance variation and dense traffic conditions.

Inference Speed. Computational efficiency has always been an important facet of object tracking within practical real-world applications. The simple convolutional architecture employed by BEVTrack ensures real-time inference at an impressive speed of 122 FPS, which is 2.72 times faster than the previously leading method, CX-Track [24]. The simplicity of BEVTrack’s pipeline facilitates flexible adjustments in model size by incorporating advanced backbones or devising more effective BMM modules to further enhance performance. This paper aims to establish a baseline model for 3D SOT and favors a lightweight structure to strike a balance between performance and efficiency. The exploration of more effective architectural designs remains a potential avenue for future research.

3.3. Ablation Studies

Design Choice of BMM Module. As detailed in Section 2.3, our approach utilizes convolutional layers with a stride of 2 to perform spatial down-sampling of features. In this ablation analysis, we aim to investigate the influence of varying the number of convolutional blocks on tracking performance. Given that each convolutional block incorporates a specific layer with a stride of 2, we characterize these different choices by their cumulative stride, denoted as $1\times$, $2\times$, $4\times$, $8\times$, and $16\times$. The results in Table 3 indicate that a $4\times$ down-sampling configuration yields the best performance. Consequently, we adopt it as the default setting.

Table 2. Comparisons with the state-of-the-art methods on NuScenes dataset.

Method	Car (64159)	Pedestrian (33227)	Truck (13587)	Trailer (3352)	Bus (2953)	mean (117278)
SC3D	22.31/21.93	11.29/12.65	35.28/28.12	35.28/28.12	29.35/24.08	20.70/20.20
P2B	38.81/43.18	28.39/52.24	48.96/40.05	48.96/40.05	32.95/27.41	36.48/45.08
BAT	40.73/43.29	28.83/53.32	52.59/44.89	52.59/44.89	35.44/28.01	38.10/45.71
GLT-T	48.52/54.29	31.74/56.49	52.74/51.43	57.60/52.01	44.55/40.69	44.42/54.33
PTTR	51.89/58.61	29.90/45.09	45.30/44.74	45.87/38.36	43.14/37.74	44.50/52.07
M2Track	55.85/65.09	32.10/60.92	57.36/59.54	57.61/58.26	51.39/51.44	49.23/62.73
BEVTrack	57.39/64.76	42.61/71.83	60.56/60.10	65.34/58.26	54.07/50.13	53.71/65.67
Improvement	$\uparrow 1.54/\downarrow 0.33$	$\uparrow 10.51/\uparrow 10.91$	$\uparrow 3.20/\uparrow 0.56$	$\uparrow 7.73/0.00$	$\uparrow 2.68/\downarrow 1.31$	$\uparrow 4.48/\uparrow 2.94$

Table 3. Ablation study of the design choice of BMM modules.

ratio	precision	success
1×	79.53	67.31
2×	81.14	69.86
4×	83.37	71.14
8×	83.22	71.27
16×	83.15	70.67

Table 4. Ablation study of the regression strategy.

Method	precision	success
Regression with l_1	82.15	69.71
Regression with l_2	80.24	68.61
Distribution-aware Regression	83.37	71.14

Table 5. Ablation study of the fusion method in BMM.

Method	precision	success
cat (c)	83.37	71.14
sum (+)	79.89	68.52
mul (×)	71.43	60.76
sub (-)	79.99	67.87

Distribution-aware Regression. To evaluate the effectiveness of the proposed distribution-aware regression strategy, a comparative analysis is conducted with conventional regression methodologies. As shown in Table 4, the distribution-aware regression approach outperforms conventional direct regression techniques, underscoring the advantages of learning the actual target translation offset distribution rather than relying on a fixed counterpart. For a qualitative examination, the learned distributions are visually represented in Fig. 3. It is noteworthy that these learned distributions exhibit a sharper central peak than the Gaussian distribution and a smoother edge compared to the

Laplace distribution. Furthermore, it is observed that these learned distributions exhibit variations across distinct categories, indicating that assuming a fixed Laplacian or Gaussian distribution is inadequate for precise tracking.

Fusion Method in BMM. We investigate various fusion techniques, specifically concatenation (denoted as 'cat (c)'), summation ('sum (+)'), multiplication ('mul (×)'), and subtraction ('sub (-)'). As shown in Table 5, concatenation yields the best performance, achieving a precision/success of 83.37/71.14. Consequently, we select concatenation as the default setting.

4. Conclusion

This paper introduces BEVTrack, a simple yet strong baseline framework for 3D single object tracking (SOT). BEVTrack performs tracking within the Bird’s-Eye View representation, thereby effectively exploiting spatial information and capturing motion cues. Additionally, we propose a distribution-aware regression strategy that learns the actual distribution of target motion, providing accurate guidance for regression. Comprehensive experiments conducted on widely recognized benchmarks underscore BEVTrack’s efficacy, establishing its superiority over state-of-the-art tracking methods. Furthermore, it achieves a high inference speed of 122 FPS. We hope this study could provide valuable insights to the tracking community and inspire further research on BEV-based 3D SOT methods.

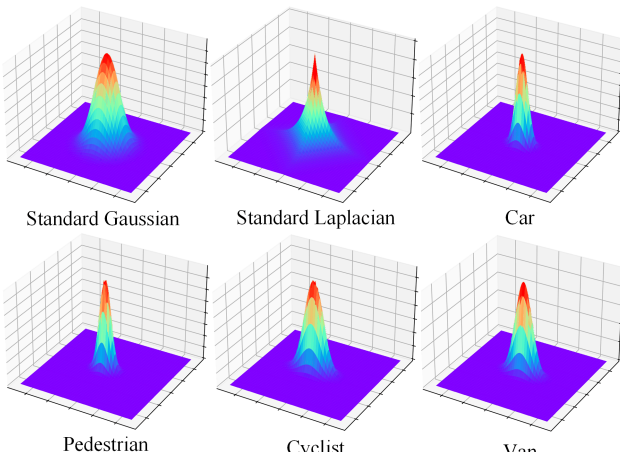


Figure 3. Visualization of the learned distributions.

References

[1] Holger Caesar, Varun Bankiti, Alex H Lang, Sourabh Vora, Venice Erin Liong, Qiang Xu, Anush Krishnan, Yu Pan, Giacarlo Baldan, and Oscar Beijbom. nuscenes: A multimodal dataset for autonomous driving. In *Proceedings of the IEEE/CVF Conference on Computer Vision and Pattern Recognition*, pages 11621–11631, 2020. [2](#), [4](#)

[2] Laurent Dinh, Jascha Sohl-Dickstein, and Samy Bengio. Density estimation using real nvp. In *International Conference on Learning Representations*, May 2016. [2](#), [3](#)

[3] Zheng Fang, Sifan Zhou, Yubo Cui, and Sebastian Scherer. 3d-siamrpn: An end-to-end learning method for real-time 3d single object tracking using raw point cloud. *IEEE Sensors Journal*, page 4995–5011, Feb 2021. [4](#)

[4] Andreas Geiger, Philip Lenz, and Raquel Urtasun. Are we ready for autonomous driving? the kitti vision benchmark suite. In *2012 IEEE Conference on Computer Vision and Pattern Recognition*, pages 3354–3361, 2012. [2](#), [4](#)

[5] Silvio Giancola, Jesus Zarzar, and Bernard Ghanem. Leveraging shape completion for 3d siamese tracking. In *2019 IEEE/CVF Conference on Computer Vision and Pattern Recognition*, Jun 2019. [4](#)

[6] Junjie Huang, Guan Huang, Zheng Zhu, Yun Ye, and Dalong Du. Bevdet: High-performance multi-camera 3d object detection in bird-eye-view. *arXiv preprint arXiv:2112.11790*, 2021. [2](#)

[7] Le Hui, Lingpeng Wang, Mingmei Cheng, Jin Xie, and Jian Yang. 3d siamese voxel-to-bev tracker for sparse point clouds. *Advances in Neural Information Processing Systems*, 34:28714–28727, 2021. [1](#), [4](#)

[8] Le Hui, Lingpeng Wang, Linghua Tang, Kaihao Lan, Jin Xie, and Jian Yang. 3d siamese transformer network for single object tracking on point clouds. In *European Conference on Computer Vision*, pages 293–310. Springer, 2022. [1](#), [2](#), [4](#)

[9] Matej Kristan, Jiri Matas, Ales Leonardis, Tomas Vojir, Roman Pflugfelder, Gustavo Fernandez, Georg Nebehay, Fatih Porikli, and Luka Cehovin. A novel performance evaluation methodology for single-target trackers. *IEEE Transactions on Pattern Analysis and Machine Intelligence*, page 2137–2155, Nov 2016. [4](#)

[10] Alex H. Lang, Sourabh Vora, Holger Caesar, Lubing Zhou, Jiong Yang, and Oscar Beijbom. Pointpillars: Fast encoders for object detection from point clouds. In *2019 IEEE/CVF Conference on Computer Vision and Pattern Recognition*, Jun 2019. [1](#)

[11] Jiefeng Li, Siyuan Bian, Ailing Zeng, Can Wang, Bo Pang, Wentao Liu, and Cewu Lu. Human pose regression with residual log-likelihood estimation. In *2021 IEEE/CVF International Conference on Computer Vision*, Oct 2021. [2](#), [3](#), [4](#)

[12] Yinhao Li, Zheng Ge, Guanyi Yu, Jinrong Yang, Zengran Wang, Yukang Shi, Jianjian Sun, and Zeming Li. Bevdepth: Acquisition of reliable depth for multi-view 3d object detection. In *Proceedings of the AAAI Conference on Artificial Intelligence*, pages 1477–1485, 2023. [2](#)

[13] Zhiqi Li, Wenhui Wang, Hongyang Li, Enze Xie, Chonghao Sima, Tong Lu, Yu Qiao, and Jifeng Dai. Bevformer: Learning bird’s-eye-view representation from multi-camera images via spatiotemporal transformers. In *European Conference on Computer Vision*, pages 1–18. Springer, 2022. [2](#)

[14] Jiahao Nie, Zhiwei He, Yuxiang Yang, Zhengyi Bao, Mingyu Gao, and Jing Zhang. Osp2b: One-stage point-to-box network for 3d siamese tracking. *arXiv preprint arXiv:2304.11584*, 2023. [4](#)

[15] Jiahao Nie, Zhiwei He, Yuxiang Yang, Mingyu Gao, and Jing Zhang. Glt-t: Global-local transformer voting for 3d single object tracking in point clouds. In *Proceedings of the AAAI Conference on Artificial Intelligence*, pages 1957–1965, 2023. [1](#), [4](#)

[16] Jonah Philion and Sanja Fidler. Lift, splat, shoot: Encoding images from arbitrary camera rigs by implicitly unprojecting to 3d. In *Computer Vision–ECCV 2020: 16th European Conference, Glasgow, UK, August 23–28, 2020, Proceedings, Part XIV 16*, pages 194–210. Springer, 2020. [2](#)

[17] Charles R Qi, Or Litany, Kaiming He, and Leonidas J Guibas. Deep hough voting for 3d object detection in point clouds. In *proceedings of the IEEE/CVF International Conference on Computer Vision*, pages 9277–9286, 2019. [1](#)

[18] Charles R Qi, Hao Su, Kaichun Mo, and Leonidas J Guibas. Pointnet: Deep learning on point sets for 3d classification and segmentation. In *Proceedings of the IEEE Conference on Computer Vision and Pattern Recognition*, pages 652–660, 2017. [1](#), [2](#)

[19] Charles Ruizhongtai Qi, Li Yi, Hao Su, and Leonidas J Guibas. Pointnet++: Deep hierarchical feature learning on point sets in a metric space. *Advances in Neural Information Processing Systems*, 30, 2017. [1](#), [2](#)

[20] Haozhe Qi, Chen Feng, Zhiguo Cao, Feng Zhao, and Yang Xiao. P2b: Point-to-box network for 3d object tracking in point clouds. In *2020 IEEE/CVF Conference on Computer Vision and Pattern Recognition*, Jun 2020. [1](#), [2](#), [4](#)

[21] Dmitry Retinskiy. Submanifold sparse convolutional networks. In *Submissions to the 2019 Kidney Tumor Segmentation Challenge: KitTS19*, Oct 2019. [2](#)

[22] Jiayao Shan, Sifan Zhou, Zheng Fang, and Yubo Cui. Ptt: Point-track-transformer module for 3d single object tracking in point clouds. In *2021 IEEE/RSJ International Conference on Intelligent Robots and Systems*, Sep 2021. [1](#), [4](#)

[23] Yue Wang, Yongbin Sun, Ziwei Liu, Sanjay E. Sarma, Michael M. Bronstein, and Justin M. Solomon. Dynamic graph cnn for learning on point clouds. *ACM Transactions on Graphics*, page 1–12, Oct 2019. [1](#), [2](#)

[24] Tian-Xing Xu, Yuan-Chen Guo, Yu-Kun Lai, and Song-Hai Zhang. Cxtrack: Improving 3d point cloud tracking with contextual information. In *Proceedings of the IEEE/CVF Conference on Computer Vision and Pattern Recognition*, pages 1084–1093, 2023. [1](#), [2](#), [4](#)

[25] Chaoda Zheng, Xu Yan, Jiantao Gao, Weibing Zhao, Wei Zhang, Zhen Li, and Shuguang Cui. Box-aware feature enhancement for single object tracking on point clouds. In *2021 IEEE/CVF International Conference on Computer Vision*, Oct 2021. [1](#), [4](#)

[26] Chaoda Zheng, Xu Yan, Haiming Zhang, Baoyuan Wang, Shenghui Cheng, Shuguang Cui, and Zhen Li. Beyond

3d siamese tracking: A motion-centric paradigm for 3d single object tracking in point clouds. In *Proceedings of the IEEE/CVF Conference on Computer Vision and Pattern Recognition*, pages 8111–8120, 2022. [1](#), [2](#), [4](#)

[27] Changqing Zhou, Zhipeng Luo, Yueru Luo, Tianrui Liu, Liang Pan, Zhongang Cai, Haiyu Zhao, and Shijian Lu. Pttr: Relational 3d point cloud object tracking with transformer. In *2022 IEEE/CVF Conference on Computer Vision and Pattern Recognition*, Jun 2022. [1](#), [2](#), [4](#)

[28] Yin Zhou, Pei Sun, Yu Zhang, Dragomir Anguelov, Jiyang Gao, Tom Ouyang, James Guo, Jiquan Ngiam, and Vijay Sudevan. End-to-end multi-view fusion for 3d object detection in lidar point clouds. In *Conference on Robot Learning*, pages 923–932. PMLR, 2020. [2](#)

[29] Yin Zhou and Oncel Tuzel. Voxelnet: End-to-end learning for point cloud based 3d object detection. In *2018 IEEE/CVF Conference on Computer Vision and Pattern Recognition*, Jun 2018. [2](#)